

Processing and analysis of MT array data from the San Andreas Fault around Parkfield, California

Wenke Wilhelms*, Michael Becken, Ute Weckmann, Oliver Ritter†

Idea

Magnetotelluric array data that were recorded by simultaneously operated instruments can be used to estimate horizontal magnetic transfer functions from the linear relation $\mathbf{H}_h^1 = \mathbf{W}\mathbf{H}_h^2$, where $\mathbf{H}_h^{1,2}$ are the horizontal magnetic fields at two sites 1 and 2 and \mathbf{W} is the 2×2 horizontal magnetic transfer function. These transfer functions can be used (I) to study induction anomalies independent of the eventually distorted electric field (II) to identify time series segments, which yield strongly disturbed estimates of the transfer function \mathbf{W} . The latter is the case, if \mathbf{W} differs considerably from an identity matrix (Ritter *et al.*, 1998).

Here, we intend to synthesize an artificial noise-free reference site for later remote reference processing. Such a synthetic dataset can be constructed from clean time series segments, identified from estimates close to the expected transfer function \mathbf{W} . Concatenation of time series segments recorded at different locations is problematic, if the spatial dependency of the magnetic fields and of \mathbf{W} is not taken into account. Therefore, we also require the full array response at all times, which we aim to reconstruct from estimated transfer functions between sites with overlapping runtimes.

The Parkfield Array data

In spring 2005, a magnetotelluric (MT) survey was undertaken to study the electric conductivity structure of the San Andreas Fault and its surroundings close to Parkfield (cf. Becken *et al.*, this volume, for a more detailed description of the survey).

Data were recorded at 41 combined broad-band and long-period sites (BMT and LMT) within a 50 km times 50 km array and an additional 40 BMT sites along a profile across the SAF. The LMT and BMT data were collected using up to 30 synchronously operated instruments (cf. Fig.1). Blue stars in Figure 1 indicate LMT sites and red circles indicate BMT sites. Light blue stars are additional LMT sites acquired in a later stage of the survey (S. Park, University of Riverside, CA). The black line marks the surface trace of the SAF according to Rymer *et al.*, (2003). The white star indicates

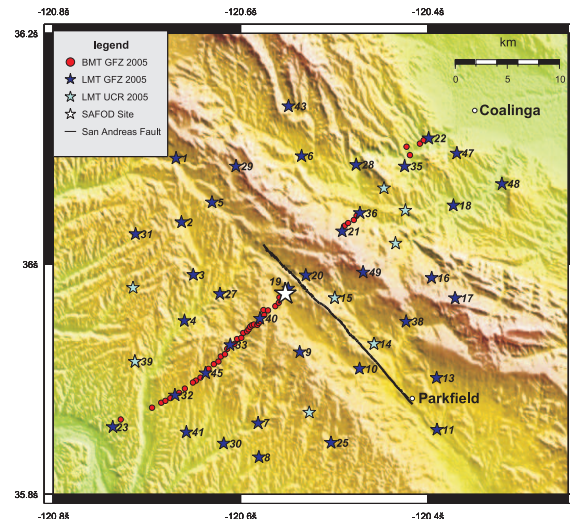


Figure 1: Regional map of the MT survey area around the SAFOD drilling site (white star) near Parkfield, California. Stars denote combined long-period/broad-band sites and red dots denote broad-band sites. The surface trace of the San Andreas Fault is indicated by a black line.

the SAFOD borehole, which is in the middle of the profile. SAFOD (**S**an **A**n*dreas **F**ault **O**bservatory at **D**epth) is part of EarthScope project. Its aim is to provide data on the composition and mechanical behaviour of a major active fault zone at depth.*

MT synchronous time series

The runtime plot in Figure 2 shows all sites and their recording times. Yellow bars mark Castle data, red bars are SPAM data and blue bars are LMT data. The recordings at the first sites start on March 19th and end on May 28th. The sampling frequency for SPAM and Castle data is 50 Hz and for LMT data it is 2 Hz. There are many synchronously operated LMT sites.

An Example of synchronously recorded 5-channel time series at seven sites are shown in Figure 3. Depicted data were recorded using two different flux-gate sensors (Lemi, Magson). Note the coherency of magnetic fields in the given time segment of 36 hours, and the phase shift and amplitude variation from site to site in the electric field.

*University of Leipzig, GFZ Potsdam

†all GFZ Potsdam

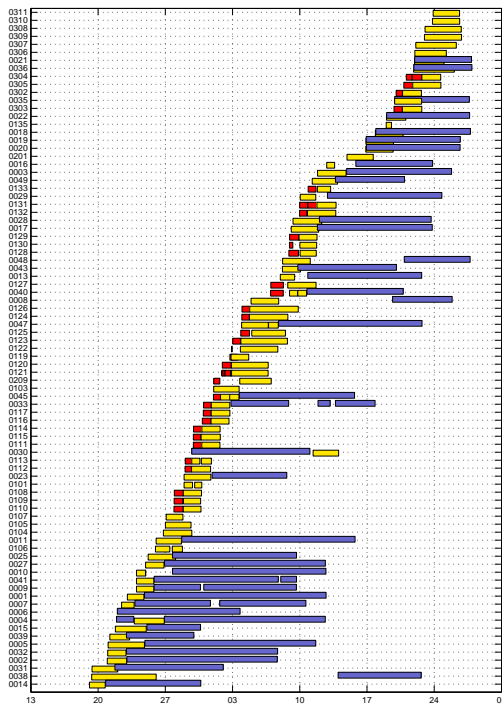


Figure 2: Run time plot of all sites; red bars are SPAM data, yellow bars are Castle (BMT) data and blue bars are LMT data.

Horizontal magnetic transfer functions

Between all simultaneously recording sites of the Parkfield array horizontal magnetic transfer functions \mathbf{W} were computed. An example of the component W_{xx} between site 4 and 5 is shown in Figure 4. This result was obtained using a single site processing (Egbert, 1986). Red symbols indicate BMT data and blue symbols mark LMT data. There is an overlap of approx. one decade between these two data types where the data match nearly perfectly. Both setups are therefore well calibrated and were working properly. If the fields at site 4 and 5 did not contain any anomalous parts, the real part of the horizontal magnetic transfer function W_{xx} would be 1 over all periods and the imaginary part would be 0 (1D earth response). In the given example, the real part of W_{xx} is highly disturbed around 10 s in the so-called dead band (low energy of MT signals).

Figure 5 shows the magnetic response function of site 4 and 5 calculated with remote reference processing (Egbert, 1986). A comparison of these results and the results of the single site processing shows an improvement of the data quality at periods around 10 s. Therefore, incorporating a clean remote reference can be extremely helpful to improve the estimation of transfer functions.

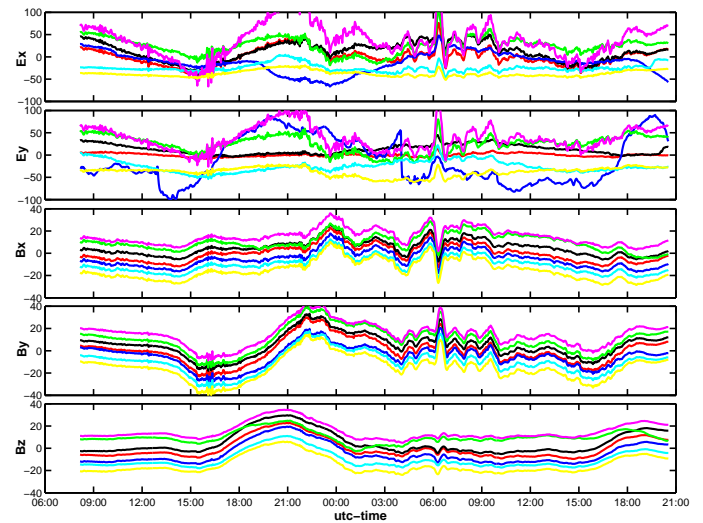


Figure 3: Time series of seven synchronously recorded sites; the first two diagrams show the electric channels E_x and E_y ; the other three are the magnetic channels B_x , B_y and B_z .

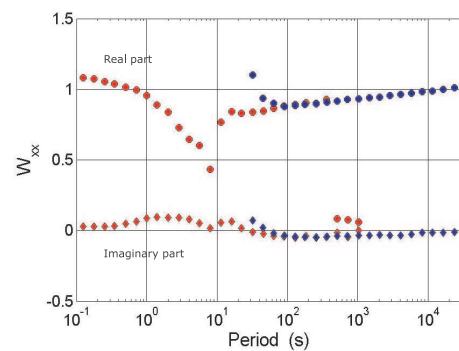


Figure 4: Results of single site processing (Egbert, 1986) of measured data, horizontal magnetic transfer function of site 4 and 5, red symbols mark BMT and blue symbols mark LMT data

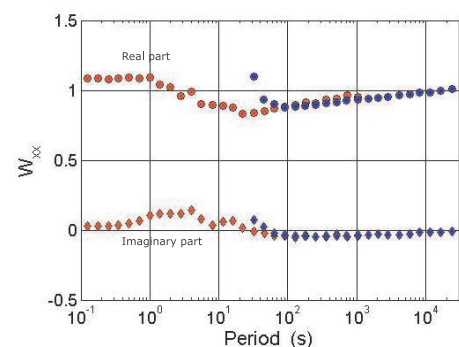


Figure 5: Horizontal magnetic transfer function after remote reference processing (Egbert, 1986) of site 4 and 5, red symbols mark BMT and blue symbols mark LMT data

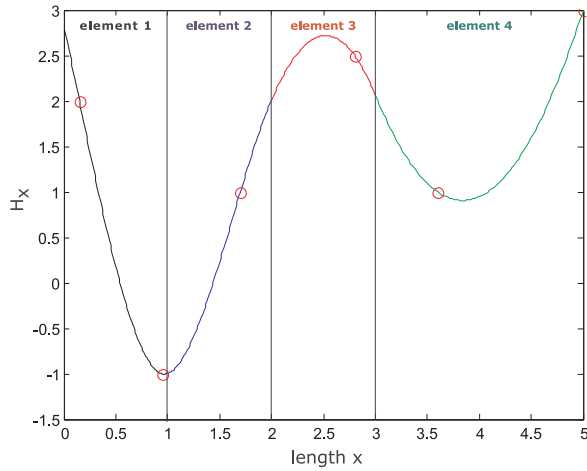


Figure 6: First approach using the finite element method in 1D and four elements - matrix \mathbf{B} is not included; red circles mark input or measured data; black, blue, red and green functions are interpolation results, they are continuous and continuously differentiable.

Interpolating magnetic fields

The induced surface magnetic field is a smooth function in space. This implies, that a smooth interpolation of measured magnetic fields is a promising approach to reconstruct the entire array response. We start our approach with the assumption, that we know the magnetic field responses at several locations due to a unit magnetic field in the x - and the y -direction. This means, that we suppose that we have estimated transfer functions between the locally recorded field and the normal field (not affected by any induction anomaly) instead of the local field at another site (which has an anomalous part). Under these circumstances, the columns of \mathbf{W} can be considered as the principal horizontal magnetic fields.

Because the magnetic field is irrotational in the air half-space, i.e. $\nabla \times \mathbf{H} = \mathbf{0}$, its horizontal components are dependent on each other via the relation

$$\frac{dH_x}{dy} = \frac{dH_y}{dx}. \quad (1)$$

Condition (1) must be satisfied by our interpolation routine.

Hence, we can formulate the following optimization problem: Find the smoothest horizontal magnetic field distribution \mathbf{H}_h , which fits the measured data to within their error bars while satisfying the relation given in equation (1).

For this purpose, we tested several functional parameterization of the magnetic field. First, we tried a *polynomial* description following an idea of Schmucker (personal communication with M. Becken). The derivatives in equation (1) are easily incorporated using a polynomial approach, which makes the use of polynomials attractive for our

problem. Though polynomials can be adequate to describe the general trend of the magnetic field such as the shape of an inhomogeneous source field, it turned out that they are not flexible enough to represent complicated responses (in the MT case and the presence of anomalies).

More complicated field distributions may be represented using piecewise polynomials, i.e. *spline functions*. With spline functions, it was however too complicated to include the relation between H_x and H_y .

Therefore, we adopted the *finite element* approach to our problem. In a first step, we reduce the problem to the 1D case to develop the formalism. Using the notation of finite elements, we formulate a variational problem of the following type: determine the magnetic field, which has minimum curvature, i.e.

$$\int H_x''(\xi)^2 d\xi = \mathbf{u}^T \mathbf{S} \mathbf{u} \rightarrow \min! \quad (2)$$

under the constraint of fitting the data and the potential field condition. Here, \mathbf{u} are the knot variables and \mathbf{S} is the stiffness matrix. In this case, we use a cubic approach, which is necessary to produce a continuously differentiable function. Measured data are collected in vector \mathbf{b} and represented in terms of the knot variables \mathbf{u} via the relation

$$\mathbf{A} \mathbf{u} = \mathbf{b} \quad (3)$$

where \mathbf{A} is a 'forward modeling operator'. Relation (1) between the derivatives of magnetic field components H_x and H_y is expressed as

$$\mathbf{B} \mathbf{u} = 0 \quad (4)$$

\mathbf{A} and \mathbf{B} depend on the ansatz functions, in this case cubic polynomials. In equation (5) these matrices are put together into one main formula that has to become minimum.

$$\mathbf{F} = \mathbf{u}^T \mathbf{S} \mathbf{u} + (\mathbf{A} \mathbf{u} - \mathbf{b})^T \lambda_1 + (\mathbf{B} \mathbf{u})^T \lambda_2 = \min. \quad (5)$$

The derivatives of (5) can be written as a product of a matrix and a vector shown in equation (7).

$$\begin{aligned} \mathbf{F}_{\mathbf{u}} &= \mathbf{S} \mathbf{u} + \mathbf{A}^T \lambda_1 + \mathbf{B}^T \lambda_2 \\ \mathbf{F}_{\lambda_1} &= \mathbf{A} \mathbf{u} - \mathbf{b} \\ \mathbf{F}_{\lambda_2} &= \mathbf{B} \mathbf{u} \end{aligned} \quad (6)$$

$$\begin{bmatrix} \mathbf{S} & \mathbf{A}^T & \mathbf{B}^T \\ \mathbf{A} & 0 & 0 \\ \mathbf{B} & 0 & 0 \end{bmatrix} \begin{bmatrix} \mathbf{u} \\ \lambda_1 \\ \lambda_2 \end{bmatrix} = \begin{bmatrix} 0 \\ \mathbf{b} \\ 0 \end{bmatrix} \quad (7)$$

Here, the vectors λ_1 and λ_2 are Lagrange multipliers, vector \mathbf{u} is the vector of coefficients that needs to be determined. Figure 6 shows the first result: fitting one component of the magnetic field using cubic functions and four elements in 1D.

Outlook

After adopting the finite element method to a problem similar to ours in 1D, it has to be developed in 2D as well to match the requirements (two magnetic field components H_x and H_y).

Dealing with measured data that contain noise, error bars have to be included in the solution (7). Moreover, to avoid oscillations in the interpolated field, a regularization trading off between data fit and smoothness constraint has to be included. Finally, not the fields directly but the transfer functions \mathbf{W} have to be incorporated iteratively, using \mathbf{W} as an initial guess for the magnetic fields themselves and $\mathbf{W}\mathbf{H}_0$ for subsequent iterations (where \mathbf{H}_0 is the reference field).

References

- Egbert, G. & Booker, J.R., 1986. Robust estimation of geomagnetic transfer functions, *Geophys. J. R. Astr. Soc.*, 87, 173-194.
- Ritter, O., Junge, A. & Dawes, G.J.K., 1998. New equipment and processing for magnetotelluric remote reference observations, *Geophys. J. Int.*, 132, 535-548.
- Rymer, M.J., Catchings, R.D. & Goldman, M.R., 2003. Structure of the San Andreas fault zone as revealed by surface geologic mapping and high-resolution seismic profiling near Parkfield, California, *Geophys. Research Abstracts*, vol.5.
- Schwarz, H.R., 1984. Methode der Finiten Elemente, B.G.Teubner Stuttgart.
- Stollnitz, E.J., Deroose, T.D. & Salesin, D.H., 1996. Wavelets for computer graphics - theory and applications, Morgan Kaufmann Publishers Inc., San Francisco, California, chapter 12.